Quantum Communication With Polarization-Encoded Qubit Using Quantum Error Correction

Daniel Barbosa de Brito, José Cláudio do Nascimento, and Rubens Viana Ramos

***Abstract*—One of the most promising physical properties for implementation of quantum technology is light polarization. However, since light polarization is a fragile property, the use of quantum error correction (QEC) is a crucial issue in order to make quantum information over optical network feasible. In this direction, this paper discusses optical setups for quantum error correction in quantum communication setups based on light polarization. In particular, we show how to use the QEC setup to provide error-free entanglement distribution and its use in an error-free probabilistic teleportation setup. Then, we discuss the performance of the error-correction setup in a very noisy channel. Finally, we show that the same QEC setup can also be used to correct bipartite of qubit states.**

***Index Terms*—Light polarization, quantum communication, quantum error correction (QEC).**

I. Introduction

QUANTUM communication and computing are new areas of information processing that make use of quantum properties in order to permit the realization of new ways of communication and computation without counterpart in the classical world, as quantum key distribution [1]–[3], quantum teleportation [4]–[6], and quantum searching [7], [8]. One of the most promising physical properties for experimental realization of quantum technologies is the light polarization. This happens because the polarization-encoded qubit is easily generated, detected, and transformed. On the other hand, it is well known that light polarization is also a fragile property that changes in an unpredictable way during light propagation in common single-mode fibers. Thus, in order to make quantum technology based on light polarization feasible, quantum error correction (QEC) schemes must be employed, that is, the unpredicted light-polarization changes must be controlled. QEC can be achieved by using quantum codes [9]–[12]. Most quantum codes are based on the introduction of redundancy. Additional qubits are included and entangled with the qubit that carries the useful information. For a polarization-encoded qubit using single-photons, each qubit is represented by the polarization of an optical pulse containing only one photon. This means that a quantum code of n qubits will use n single-photon pulses, where $n-1$ are ancillas. The n photons must be entangled through an n-qubit quantum circuit. All of them are sent through a noisy channel and disentangled at the receiver by another quantum circuit. The ancillas are measured and, according to their values, a selected single-qubit operation (a polarization change) is applied in the signal qubit in order to recover the correct polarization. The block diagram is shown in Fig. 1. In this figure, $|\theta\rangle$ is the input signal and $|\theta'\rangle$ is the corrupted signal at channel output. The ancillas are considered initially in the horizontal linear polarization.

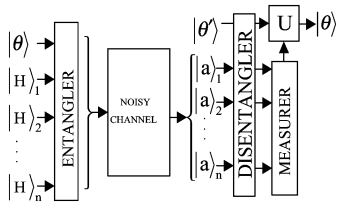

Fig. 1. QEC using entangled states.

The most famous quantum code able to correct a general single-qubit error is the Shor code [13]. It uses nine qubits. The smallest quantum code able to correct a general error in a qubit is a five-qubits code [13]. The codification, using unnormalized states, is given as

$$\begin{aligned}|0_L\rangle = {} & |HHHHH\rangle + |VHHVH\rangle + |HVHHV\rangle \\ & + |VHVHH\rangle + |HVHVH\rangle - |VVHVV\rangle \\ & - |HHVVH\rangle - |VVHHH\rangle - |VVVHV\rangle \\ & - |HHHVV\rangle - |VVVVH\rangle - |HVVVV\rangle \\ & - |VHHHV\rangle - |HVVHH\rangle - |VHVVV\rangle \\ & + |HHVHV\rangle \end{aligned} \tag{1}$$

$$\begin{aligned}|1_L\rangle = {} & X|0_L\rangle = |VVVVV\rangle + |HVVHV\rangle + |VHVVH\rangle \\ & + |HVHVV\rangle + |VHVHV\rangle - |HHVHH\rangle \\ & - |VVHHV\rangle - |HHVVV\rangle - |HHHVH\rangle \\ & - |VVVHH\rangle - |HHHHV\rangle - |VHHHH\rangle \\ & - |HVVVH\rangle - |VHHVV\rangle - |HVHHH\rangle \\ & + |VVHVH\rangle . \end{aligned} \tag{2}$$

In (2), X is a polarization rotator of $\pi/2$ (the NOT gate). The quantum coder and decoder is the quantum circuit shown in Fig. 2 [14].

In Fig. 2, Z, Y, and H are the (single-qubit gates) polarization rotations

$$Z = \begin{bmatrix} 1 & 0 \\ 0 & -1 \end{bmatrix}; Y = \begin{bmatrix} 0 & -i \\ i & 0 \end{bmatrix}; H = \frac{1}{\sqrt{2}} \begin{bmatrix} 1 & 1 \\ 1 & 1 \end{bmatrix}. \tag{3}$$

The controlled gates are gates that are applied only if the control qubit (indicated by a black ball) is in the vertical polarization. For example, in the third column of Fig. 2, a Y gate will

Manuscript received March 21, 2007; revised September 17, 2007.

The authors are with the Department of Teleinformatic Engineering, Federal University of Ceará, 60755-640 Fortaleza Ceará, Brazil (e-mail: rubens@deti.ufc.br).

Color versions of one or more of the figures in this paper are available online at http://ieeexplore.ieee.org.

Digital Object Identifier 10.1109/JQE.2007.911689

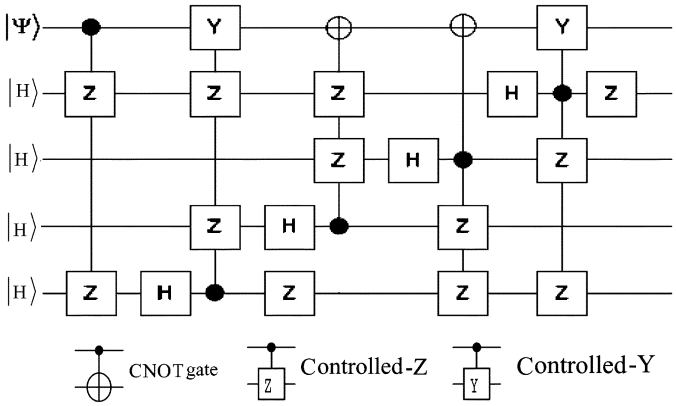

Fig. 2. Quantum circuit for five-qubit quantum code.

be applied in the first qubit and a Z gate will be applied in the second and fourth qubits only if the fifth qubit is vertical. Every single-qubit gate can be implemented using polarization rotators and compensators. On the other hand, the two-qubit gates Controlled-NOT (CNOT) and Controlled $-Z$ require large nonlinearities, not achievable with present optical materials. A CNOT gate using only linear optical device can be constructed; however, its behavior is probabilistic: sometimes the gate works and sometimes it fails [15]–[18]. Therefore, the physical implementation of quantum codes employing redundancy through entanglement is, with current technology, inefficient. On the other hand, a single-qubit QEC system that does not use both ancillas and entanglement has been proposed [18]. Hence, this scheme can be built with today's technology. In this direction, this paper extends the schemes proposed in [19] and [20] in three ways: 1) proposing a complete optical setup for probabilistic quantum teleportation using QEC; 2) analyzing the performance of the QEC setup when the channel is very noisy due to fast variations of the fiber birefringence; and 3) showing that the QEC setup can also be used to protect bipartite of qubit quantum states.

This paper is outlined as follows. In Section II, the QEC setup for single-photon quantum communication systems and its use in error-free entanglement distribution and probabilistic teleportation are considered. In Section III, the performance of the QEC setup considering a very noisy channel is analyzed. In Section IV, we show that the QEC setup can also be used to correct bipartite of qubit quantum states. Finally, the conclusions are presented in Section V.

II. QEC Setups

In order to make the polarization-encoded qubit transmission protected against the noise (unpredictable polarization rotations) during fiber propagation, quantum codes can be used. However, a simpler QEC (without using ancillas and entanglement) based on a time-bin qubit has been proposed [19] as well its use in error-free distribution of a polarization-entangled pair of photons [21]. A simplified version of the setup presented in [19] was proposed in [20]. Here, we show this last is also suitable for error correction in polarization entangled pair of photons distribution. First, we give a brief description of the optical setup used, which is shown in Fig. 3 [20].

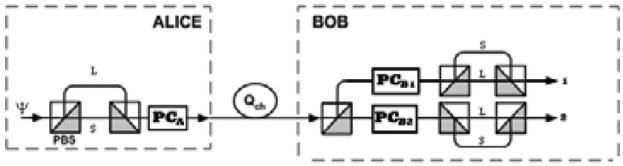

Fig. 3. Optical setup for error correction.

In Fig. 3, PCs are Pockels cells and L and S are, respectively, long and short paths. Let us assume that the input state at Alice's place is $|\psi\rangle = \alpha|H\rangle + \beta|V\rangle$ and the noisy channel is modeled by the unitary operation U that implements the transformation

$$U|H\rangle = \cos(\varphi)|H\rangle + \sin(\varphi)e^{i\lambda}|V\rangle \tag{4}$$

where φ and λ are random variables. In Fig. 3, there are two paths after the first PBS, a short path (S) taken by the horizontal component and a long path (L) taken by the vertical component. When the input state passes through the unbalanced polarization interferometer, the components of the polarization are separated in time, producing the state $\alpha|H\rangle_S + \beta|V\rangle_L$. Alice turns on her Pockels cell only when the L component is present, effecting the transformation $|V\rangle_L \rightarrow |H\rangle_L$. Thus, the encoded state sent by Alice in the quantum channel is $|\Psi\rangle = \alpha|H\rangle_S + \beta|H\rangle_L$. Using (4), the quantum state at channel output is given by

$$\begin{aligned} U|\Psi\rangle =& \alpha\left(\cos(\varphi)|H\rangle_S + e^{i\lambda}\sin(\varphi)|V\rangle_S\right) \\ &+ \beta\left(\cos(\varphi)|H\rangle_L + \sin(\varphi)e^{i\lambda}|V\rangle_L\right). \end{aligned} \tag{5}$$

At Bob's side, the Pockels cell PC_{B1} is activated to rotate the polarization only of the S component while PC_{B2} is activated to rotate only the L component. At each mode 1 (upper arm) and 2 (lower arm), there exists an unbalanced polarization interferometer. In these interferometers, the horizontal component takes the long path while the vertical component takes the short path. When the corrupted state (5) arrives at Bob's place, after passing through the first PBS and Pockels cells, it is transformed to

$$\begin{aligned} &\alpha\left[\cos(\varphi)|H\rangle_S^2 + \sin(\varphi)e^{i\lambda}|H\rangle_S^1\right] \\ &\quad+\beta\left[\cos(\varphi)|V\rangle_L^2 + \sin(\varphi)e^{i\lambda}|V\rangle_L^1\right]. \end{aligned} \tag{6}$$

This state passes through the unbalanced polarization interferometers producing the total output state

$$\begin{aligned} &\cos(\varphi)\left(\alpha|H\rangle_{SL}^2 + \beta|V\rangle_{LS}^2\right) \\ &\quad+\sin(\varphi)e^{i\lambda}\left(\alpha|H\rangle_{SL}^1 + \beta|V\rangle_{LS}^1\right). \end{aligned} \tag{7}$$

In (6) and (7), the superscripts 1 and 2 denote the paths towards the output modes 1 and 2. From (7), one sees that Bob obtains the corrected state in outputs 1 and 2 with probabilities, respectively, equal to $\sin^2(\varphi)$ and $\cos^2(\varphi)$. When the channel is approximately an ideal channel, Bob obtains the uncorrupted state that is more likely in output 1, on the other hand, when φ is allowed to vary over its total range of values according to a uniform distribution, then the probability of obtaining the uncorrupted state in one of the outputs tends to 1/2. One cannot be sure in which output the photon will emerge, however, using

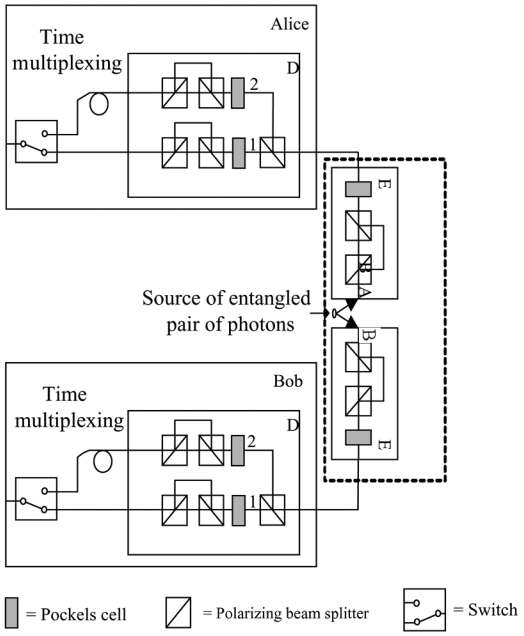

Fig. 4. Error-correction setup for a polarization-entangled pair of protons.

an optical delay and an electrooptic switch to form a time-multiplexing system, one can have the photon always at the same output (but in different times).

Any error (polarization change) that can be modeled by the sequence compensator–rotator–compensator can be corrected. For this, the characteristic time of change of the fiber parameters must be larger than the time separation between S and L pulses. It is important to note that the setup shown in Fig. 3 can also work well for coherent states and, hence, it can also be used for passive polarization correction in classical optical communication systems.

Using two equal setups of the type shown in Fig. 3, the setup for error correction in Bell state distribution is as shown in Fig. 4.

In Fig. 4, the time-multiplexing scheme composed by a time delay and an electrooptic switch is used to guarantee that both photons will always emerge from the same output at Alice's side and Bob's side. It is easy to show that, having the initial input state $|\Phi\rangle = [|HH\rangle + |VV\rangle]/2^{1/2}$, the output state is

$$|\Phi\rangle = \sum_{j,k=1}^{2} e^{i\xi_{jk}} \sin\left(\varphi_a - \frac{j\pi}{2}\right) \sin\left(\varphi_b - \frac{k\pi}{2}\right) |\phi\rangle_{jk} \quad (8)$$

$$|\phi\rangle_{jk} = \frac{|HH\rangle_{jk} + |VV\rangle_{jk}}{\sqrt{2}} \quad (9)$$

$$\begin{aligned} \xi_{11} &= \phi_a + \phi_b \\ \xi_{12} &= \phi_a + \lambda_b \\ \xi_{21} &= \lambda_a + \phi_b \\ \xi_{22} &= \lambda_a + \lambda_b \end{aligned} \quad (10)$$

where the noisy channels (channel a: from the source of entangled photons to Alice; channel b: from the source of entangled photons to Bob) are modeled by the unitary operations realizing the transformations $U_{a(b)}|H\rangle = \cos(\varphi_{a(b)})e^{i\phi a(b)}|H\rangle + \sin(\varphi_{a(b)})e^{i\lambda a(b)}|V\rangle$ (again, the angles

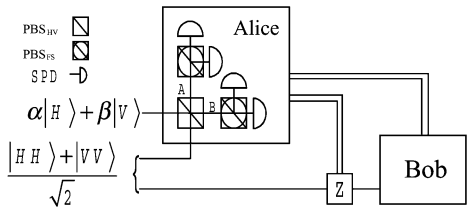

Fig. 5. Optical setup for probabilistic teleportation of polarization-encoded qubit.

are random variables). The state $|HH\rangle_{jk}$, for example, means a horizontal state emerging from output $j(k)$ at Alice (Bob). After the time multiplexing, the spatial uncertainty becomes a time uncertainty, that is, the photon will appear earlier if it took the shortest path (output 1) or the latter if it took the longest path (output 2). Once entangled photons can be distributed in an error-free way, it is possible to construct quantum communication with a low error rate.

A probabilistic teleportation of polarization-encoded qubit can be implemented using the setup shown in Fig. 5 [22].

In Fig. 5, SPD is a single-photon detector, PBS_{HV} is a polarization beam splitter (PBS) in the rectangular basis $\{|H\rangle, |V\rangle\}$, while PBS_{FS} is a PBS in the diagonal basis $\{|F\rangle = [|H\rangle + |V\rangle]/2^{1/2}, |S\rangle = [|H\rangle - |V\rangle]/2^{1/2}\}$. The double lines mean classical communication. The quantum state evolution in the setup in Fig. 5 is as follows:

$$|\psi\rangle_{\mathrm{in}} = (\alpha|H\rangle + \beta|V\rangle)\left(\frac{|HH\rangle + |VV\rangle}{\sqrt{2}}\right) \quad (11)$$

$$|\psi\rangle_{\mathrm{PBS}_{HV}} = \frac{1}{\sqrt{2}}[\alpha|HHH\rangle + \beta|VVV\rangle] + \frac{1}{\sqrt{2}}|\Omega\rangle \quad (12)$$

$$|\Omega\rangle = \alpha|HV, 0, V\rangle + \beta|0, VH, H\rangle \quad (13)$$

$$\begin{aligned} |\psi\rangle_{\mathrm{PBS}_{FS}} = &\frac{1}{\sqrt{2}} \\ &\times \frac{(|FF\rangle + |SS\rangle)|\Psi^+\rangle + (|FS\rangle + |SF\rangle)|\Psi^-\rangle}{2} \\ &+ \frac{1}{\sqrt{2}}|\Omega\rangle \end{aligned} \quad (14)$$

$$|\Psi^{\pm}\rangle = \alpha|H\rangle \pm \beta|V\rangle. \quad (15)$$

The teleportation succeeds if Alice measures one photon in output A and one photon in output B. Hence, as can be seen in (14) and (15), Alice has to send two classical bits to Bob, the first one informing if the teleportation succeeded, which happens with a probability of 50%, and the second informing if Bob does or does not have to apply a phase shift in his photon.

Now, it is possible to put the setups shown in Figs. 4 and 5 together in order to construct an optical setup for probabilistic quantum teleportation employing error correction and using only simple optical devices. The setup proposed is shown in Fig. 6. Using it, a quantum teleportation succeeds with probability $0.25\cos^2(\varphi_a)$ if Bob just measures the qubit received. The probability $\cos^2(\varphi_a)$ appears due to the fact that Alice sends the qubit $|\phi_{\mathrm{in}}\rangle$ at the right time to coincide with the arrival of the photon that took path 1. If the photon coming from the central node took path 2, the teleportation does not happen. If Bob uses the qubit received to another quantum operation for which he has to know the exact time of arrival

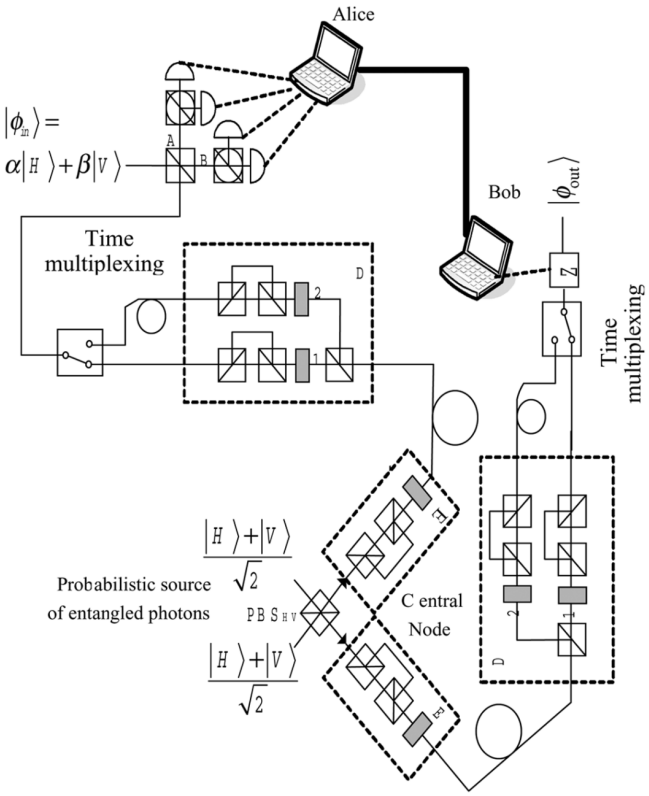

Fig. 6. Simple optical setup for probabilistic teleportation employing error correction.

of the photon sent by the central node, then the probability of success is $0.25\cos^2(\varphi_a)\cos^2(\varphi_b)$, assuming that Bob also realizes his synchronization considering output 1.

III. Very Noisy Channel

Here, we analyze the performance of the error-correction setup when the channel is very noisy, implying that the fiber birefringence has fast variations and it can change during the time interval between the short and long time slots. In this case, the pulses in each time slot will experiment different unitary evolutions. Since the channel varies between the S and L components of the state sent by Alice, what is the probability of the state received by Bob to be the same as that sent by Alice? In order to answer this question, consider that $U_S(\varphi_S, \xi_S, \lambda_s)$ and $U_L(\varphi_L, \xi_L, \lambda_L)$ are, respectively, the unitary transformations acting in the S and L pulses. The quantum state at Alice's encoder output can be represented by

$$\alpha|H,S\rangle+\beta|H,L\rangle=|H\rangle(\alpha|S\rangle+\beta|L\rangle). \tag{16}$$

Hence, polarization and time-bin are not entangled. When the unitary transformation is the same for both pulses, the channel does not entangle polarization and time-bin and the qubit can be received corrected at the receiver. On the other hand, when the fiber birefringence varies in a time interval shorter than the time separation between S and L pulses, one has at channel output

$$\begin{aligned}\alpha U_S|H,S\rangle+\beta U_L|H,L\rangle=&\\ \alpha\cos(\varphi_S)|H,S\rangle+\alpha\sin(\varphi_S)e^{i\lambda_S}|V,S\rangle&\\ +\beta\cos(\varphi_L)|H,L\rangle+\beta\sin(\varphi_L)e^{i\lambda_L}|V,L\rangle&\end{aligned} \tag{17}$$

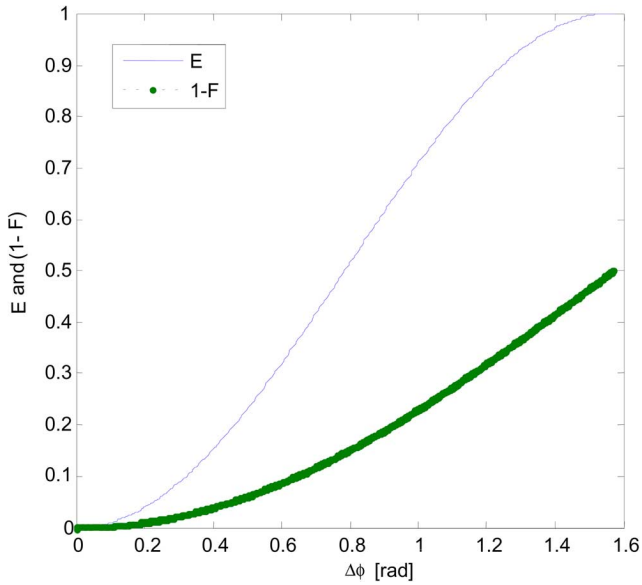

Fig. 7. Error rate and entanglement versus $\Delta\Phi=\varphi_L-\varphi_s$ when $\lambda_L=\lambda_s$.

and polarization and time-bin are entangled. The amount of entanglement of the state (18) is given by

$$\begin{aligned}E=&4|\alpha|^2|\beta|^2\left|\langle V|U_S^{\dagger}U_L|H\rangle\right|^2\\ =&4|\alpha|^2|\beta|^2\Delta_1\end{aligned} \tag{18}$$

$$\begin{aligned}\Delta_1=&\cos^2(\varphi_S)\sin^2(\varphi_L)+\cos^2(\varphi_L)\sin^2(\varphi_S)\\ &-2\cos(\varphi_S)\sin(\varphi_L)\cos(\varphi_L)\sin(\varphi_S)\cos(\lambda_L-\lambda_S).\end{aligned} \tag{19}$$

As expected, when $U_S=U_L$, one has $U_S^{\dagger}U_L=I$, resulting in $E=0$, and the QEC does not fail. The output state is

$$\begin{aligned}|\psi\rangle=&\sin(\varphi_S)e^{i\lambda_S}\alpha|H\rangle_{SL}^1+\sin(\varphi_L)e^{i\lambda_L}\beta|V\rangle_{SL}^1\\ &+\cos(\varphi_S)\alpha|H\rangle_{SL}^2+\cos(\varphi_L)\beta|V\rangle_{SL}^2\end{aligned} \tag{20}$$

and its fidelity is given by

$$F=|\alpha|^4+|\beta|^4+2|\alpha|^2|\beta|^2\Delta_2 \tag{21}$$

$$\Delta_2=\cos(\varphi_S)\cos(\varphi_L)+\sin(\varphi_S)\sin(\varphi_L)\cos(\lambda_L-\lambda_S). \tag{22}$$

The larger the entanglement, the larger the error rate $1-F$. This can be seen in the simple case that $\lambda_L=\lambda_S$. In this case, Δ_1 and Δ_2 depend only on $\Delta\Phi=\varphi_L-\varphi_S$, and one can obtain the curve shown in Fig. 7 for $|\alpha|^2|\beta|^2=0.5$.

For other values of $|\alpha|^2$ and $|\beta|^2$, the same kind of behavior is observed.

IV. Beyond Qubit Error Correction

In Section II, it was shown how to use the QEC setup to protect the individual qubits of a bipartite state, that is, each individual qubit "sees" a different channel. Here, we consider the correction of the complete bipartite state. In other words, Alice has the bipartite state $|\Psi\rangle=\alpha|HH\rangle_{0\delta}+\beta|HV\rangle_{0\delta}+\gamma|VH\rangle_{0\delta}+\xi|VV\rangle_{0\delta}$ that are two photons separated by δ in time, and she

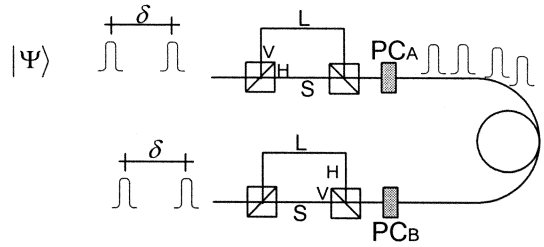

Fig. 8. QEC of bipartite quantum state.

wants to send this state to Bob. In order to do this, Alice uses the setup shown in Fig. 8.

The quantum state leaving Alice's polarization interferometer and after Alice's Pockels cell are respectively

$$|\psi_1\rangle = \alpha|HH\rangle_{S,\delta S} + \beta|HV\rangle_{S,\delta L} + \gamma|VH\rangle_{L,\delta S} + \xi|VV\rangle_{L,\delta L} \quad (23)$$

$$|\psi_2\rangle = \alpha|HH\rangle_{S,\delta S} + \beta|HH\rangle_{S,\delta S} + \gamma|HH\rangle_{L,\delta S} + \xi|HH\rangle_{L,\delta L}. \quad (24)$$

In (24), one can observe that there are four time slots: S, $\delta+S$, L, and $\delta+L$. As can be noted in (24), PC_A is activated in order to rotate the polarization $(\pi/2)$ of the pulses only in the time slots L and $\delta+L$. Once more, channel propagation is modeled by an unknown unitary transformation, but now this one acts in both qubits. In a general way, one can say that $U|HH\rangle = a|HH\rangle + b|HV\rangle + c|VH\rangle + d|VV\rangle$, where the coefficients a, b, c, and d depend on the parameters of U. Thus, the quantum state at channel output is

$$\begin{aligned}|\psi_3\rangle = {} & a(\alpha|HH\rangle_{S,\delta S} + \beta|HH\rangle_{S,\delta L} + \gamma|HH\rangle_{L,\delta S} + \xi|HH\rangle_{L,\delta L}) \\ & + b(\alpha|HV\rangle_{S,\delta S} + \beta|HV\rangle_{S,\delta L} + \gamma|HV\rangle_{L,\delta S} + \xi|HV\rangle_{L,\delta L}) \\ & + c(\alpha|VH\rangle_{S,\delta S} + \beta|VH\rangle_{S,\delta L} + \gamma|VH\rangle_{L,\delta S} + \xi|VH\rangle_{L,\delta L}) \\ & + d(\alpha|VV\rangle_{S,\delta S} + \beta|VV\rangle_{S,\delta L} + \gamma|VV\rangle_{L,\delta S} + \xi|VV\rangle_{L,\delta L}). \end{aligned} \quad (25)$$

Now, Bob activates his Pockles cell in order to rotate the polarization only of the pulses in the time slots L and $\delta+L$. Further, in Bob's polarization interferometer, the horizontal component takes the longest path while the vertical component takes the shortest path. Thus, Bob's output state is

$$\begin{aligned}|\psi_4\rangle = {} & a(\alpha|HH\rangle_{SL,\delta SL} + \beta|HV\rangle_{SL,\delta LS} + \gamma|VH\rangle_{LS,\delta SL} + \xi|VV\rangle_{LS,\delta LS}) \\ & + b(\alpha|HV\rangle_{SL,\delta SS} + \beta|HH\rangle_{SL,\delta LL} + \gamma|VV\rangle_{LS,\delta SS} + \xi|VH\rangle_{LS,\delta LL}) \\ & + c(\alpha|VH\rangle_{SS,\delta SL} + \beta|VV\rangle_{SS,\delta LS} + \gamma|HH\rangle_{LL,\delta SL} + \xi|HV\rangle_{LL,\delta LS}) \\ & + d(\alpha|VV\rangle_{SS,\delta SS} + \beta|VH\rangle_{SS,\delta LL} + \gamma|HV\rangle_{LL,\delta SS} + \xi|HH\rangle_{LL,\delta LL}). \end{aligned} \quad (26)$$

As can be seen in (26), there are six time slots at the output: $S+S$, $S+S+\delta$, $S+L$, $S+L+\delta$, $L+L$, and $L+L+\delta$. With probability $|a|^2$, the correct state is found in the time slots $S+L$ and $S+L+\delta$. Hence, selecting only these two time slots, one can be sure that, if there are photons, then they represent the correct bipartite state.

V. Conclusion

We have discussed an error-correction setup based on a time-bin qubit showing how to use it to obtain error-free entanglement distribution. Then the complete setup for probabilistic teleportation of polarization-encoded qubit with error correction for entanglement distribution was presented. The advantage of this setup is the fact that it uses only linear optical devices and, hence, it can be constructed with today's technology. The difficulties in the setup proposed are the time synchronization due to the Pockels cell in the error-correction setup and the fact that the polarization interferometers at the transmitter and receiver must be equal. It also suffers from other problems that are common to every setup for quantum communication in optical networks, like the low performance of present single-photon detectors and single-photon sources. Furthermore, it is assumed that, when the Pockels cell is not active, it does not introduce any change in the polarization of the pulse passing through it. Hence, we assume that horizontally polarized photons are not disturbed. In the real device, however, this may not be the case, and some error may be introduced into the system. However, it is possible to place a compensator–rotator–compensator after the Pockels cell just to compensate for its behavior in the best way. Moreover, the coupling between an optical fiber and nonfiber-based optical devices always implies loss. This loss does not cause an error, but it decreases the probability of the photon to arrive at the receiver's place. Then, it was shown that, if the channel varies during the time interval between the first and second time slots, then an entanglement between the photon polarization and time slot arises. In this case, the performance (ability to correct the polarization change during fiber propagation) of the error-correction setup depends on the amount of entanglement between polarization and time-bin. The larger the entanglement, the larger the error rate, although this last also depends on the polarization qubit sent. At last, we showed that the optical setup used to correct single-qubit error can also de used to correct the error of a bipartite of the qubit state.

There is an error-detection technique called error filtration [23], [24]. It is quite interesting, but it does not seem to be better than the techniques proposed in [19] and [20], because it is still possible to find errors in the "useful output" in the error filtration. On the other hand, in the setups proposed in [19], [20], and in this study, only corrected qubits (in the case that both components of the time-bin qubit experiment the same channel) emerge at the "useful output."

As explained in the text, our setups transform the polarization-encoded qubit to a time-bin qubit, since the latter is more robust against polarization fluctuation. A question that may arise is: why should one construct quantum communication systems based on light polarization instead of constructing quantum communication systems based only in time-bin

qubits? Some answers are: 1) the existing quantum memories work with polarization qubit [25] and 2) quantum computation with linear optical devices has been proposed with polarization qubits [15]–[18]. Hence, for the realization of nonlocal quantum computation over optical networks (for example, a nonlocal CNOT), polarization-encoded qubit is important. What our schemes (and those in [19] and [20]) do, in fact, is to transform polarization qubits into time-bin qubits only for fiber propagation. At the receiver, the time-bin qubits are transformed to polarization qubit again. However, one knows that in the correct time slots there will not be any error on the qubit.

Finally, it is important to note that active channel equalization can also be applied for QEC in quantum communication systems based on light polarization. In this kind of error correction, from time to time, optical pulses are sent through the fiber and their polarizations at the fiber output are measured in order to find the correct compensator–rotator–compensator values that implement the inverse transfer function of the channel. For our setups, however, this is not necessary. It will always work. Thus, our setups are passive in the sense that it is not necessary to find out which are the channel's parameters in order to adjust an equalizer.

REFERENCES

[1] C. H. Bennet, "Quantum cryptography using any two nonorthogonal states," *Phys. Rev. Lett.*, vol. 68, no. 21, pp. 3121–3124, 1992.

[2] N. Gisin, G. Ribordy, W. Tittel, and H. Zbinden, "Quantum cryptography," *Rev. Mod. Phys.*, vol. 74 145, pp. 145–195, 2002.

[3] C. H. Bennett and G. Brassard, "1984 quantum cryptography: Public key distribution and coin tossing proc. IEEE," in *Proc. Conf. Comput. Syst. Signal Process.*, 1992, pp. 175–179.

[4] C. H. Bennett, G. Brassard, C. Crépea, R. Jozsa, A. Peres, and W. K. Wootters, "Teleporting an unknown quantum state via dual classical and Einstein-Podolsky-Rosen channels," *Phys. Rev. Lett.*, vol. 70, pp. 1895–1898, 1993.

[5] A. Zeilinger, "Quantum entanglement: A fundamental concept finding its applications," *Phys. Scripta*, vol. T76, pp. 203–209, 1998.

[6] C. H. Bennett, "Quantum information," *Phys. Scripta*, vol. T76, pp. 210–217, 1998.

[7] L. K. Grover, "A fast quantum mechanical algorithm for database search," in *Proc. 28th Annu. ACM Symp. Theory Computing*, Philadelphia, PA, 1996, pp. 212–219.

[8] A. Barenco, "Quantum physics and computers," *Contemp. Phys.*, vol. 37, no. 5, pp. 375–389, 1996.

[9] M. Grassl, T. Beth, and M. Roetteler, "On optimal quantum codes," *Int. J. Quantum Inf.*, vol. 2, no. 1, pp. 55–64, 2004.

[10] D. Kribs, R. Laflamme, and D. Poulin, "Unified and generalized approach to quantum error correction," *Phys. Rev. Lett.*, vol. 94, p. 180501/1–4, 2005.

[11] B. Schumacher, "Quantum coding," *Phys Rev. A*, vol. 51, no. 4, pp. 2738–2747, 1995.

[12] A. Steane, "Quantum computing," *Rep. Prog. Phys.*, vol. 61, pp. 117–173, 1998.

[13] M. A. Nielsen and I. L. Chuang, *Quantum Computation and Quantum Information*. Cambridge, U.K.: Cambridge Univ. Press, 2000.

[14] R. Baumann, "Quantum error correction," Department of Physics, Institute for Theoretical Physics, Swiss Federal Institute of Technology ETH, Zurich, Switzerland, 2003 [Online]. Available: http://e-collection.ethbib.ethz.ch/

[15] T. B. Pitman, B. C. Jacobs, and J. D. Franson, "Experimental demonstration of a quantum circuit using linear optics gates," *Phys. Rev. A*, vol. 71, p. 032307/1–4, 2005.

[16] F. M. Spedalieri, H. Lee, and J. P. Dowling, "High-fidelity linear optical quantum computing with polarization encoding," *Phys. Rev. A*, vol. 73, p. 012334/1–11, 2006.

[17] T. C. Ralph, A. G. White, W. J. Munro, and G. J. Milburn, "Simple scheme for efficient linear optics quantum gates," *Phys. Rev. A*, vol. 65, p. 012314/1–6, 2001.

[18] P. Kok, W. J. Munro, K. Nemoto, T. C. Ralph, J. P. Downling, and G. J. Milburn, Review Article: Linear Optical Quantum Computing 2005, quant-ph/0512071.

[19] D. Kalamidas, "Single-photon quantum error rejection and correction with linear optics," *Phys. Lett. A*, vol. 343, pp. 331–335, 2005.

[20] J. C. do Nascimento, F. A. Mendonça, and R. V. Ramos, "Linear optical setups for active and passive quantum error correction in polarization encoded qubits," *J. Mod. Opt.*, vol. 54, no. 10, pp. 1467–1479, 2007.

[21] D. Kalamida, "Linear optical scheme for error-free entanglement distribution and a quantum repeater," *Phys. Rev. A*, vol. 73, p. 054304/1–3, 2006.

[22] D. B. de Brito, J. B. R. Silva, and R. V. Ramos, "Optical setups for probabilistic bipartite and tripartite entanglement generation and quantum teleportation in optical networks," *J. Mod. Opt.*, to be published.

[23] N. Gisin, N. Linden, S. Massar, and S. Popescu, "Error filtration and entanglement purification for quantum communication," *Phys. Rev. A*, vol. 72, p. 012338/1–17, 2005.

[24] L.-P. Lamoureux, E. Brainis, N. J. Cerf, P. Emplit, M. Haelterman, and S. Massar, "Experimental error filtration for quantum communication over highly noisy channels," *Phys. Rev. Lett.*, vol. 94, p. 230501/1–4, 2005.

[25] D. FelintoC. W. ChouJ. LauratE. W. SchomburgH de RiedmattenH. J. Kimble, "Conditional control of the quantum states of remote atomic memories for quantum network," *Nature Phys.*, vol. 2, pp. 844–848, 2006.

Daniel Barbosa de Brito was born in Fortaleza, Brazil. He received the B.A. degree in electrical engineering and the M. Phil. degree in teleinformatic engineering from Federal University of Ceará, Ceará, Brazil, in 2005 and 2007, respectively. He is currently working toward the Ph.D. degree in quantum information at the Department of Teleinformatic Engineering, Federal University of Ceará.

José Cláudio do Nascimento was born in Fortaleza, Brazil. He received the B.A. degree in electrical engineering and the M. Phil. degree in teleinformatic engineering from Federal University of Ceará, Ceará, Brazil, in 2005 and 2006, respectively. He is currently working toward the Ph.D. degree in quantum information at the Department of Teleinformatic Engineering, Federal University of Ceará.

Rubens Viana Ramos was born in Fortaleza, Brazil. He received the B.A. degree from Federal University of Ceará, Ceará, Brazil, in 1996, and the M. Phil. and Ph.D. degrees from the State University of Campinas, São Paulo, Brazil, in 1998 and 2000, respectively, all in electrical engineering.

He was a Postdoctoral Researcher with the Royal Institute of Technology, Sweden, in 2001 and he is currently a Professor of quantum information and optics communication with the Department of Teleinformatic Engineering, Federal University of Ceará, Ceará, Brazil. He has published more than 30 technical papers in quantum information and optical communication areas in peer-reviewed scientific journals.